New Robotic Architecture for NDT Applications

Martin Švejda [*]

[*] *Department of Cybernetics, University of West Bohemia, Pilsen,*
Czech Republic (e-mail: msvejda.kky.zcu.cz).

Abstract: The paper deals with the new architecture of the 4 degrees of freedom manipulator for Non-Destructive Testing (NDT) of the pipe welds of complex geometries. The main contribution is to overcome the known disadvantages resulting from using standard robotic architectures (universal industrial or single purposes special manipulators) regarding e.g. space requirements or limited applicability. The direct and inverse kinematic is solved. The singularity configuration analysis of the manipulator is derived in the sense of finding implicit description of the varieties in the task space. It makes possible to easily deal with singular configurations during the end-effector trajectory planning. In order to use the proposed manipulator for NDT of pipe welds the trajectory generators are introduced. The circumferential, elbow, longitudinal and branch weld are taken into account. It is shown that the trajectory parametrization of the first three types of welds can be found easily. But for the branch weld there are some drawbacks regarding unnatural parametrization of the branch weld primitives (ellipses, Steinmetz solid). Therefore the new numerical algorithm is developed and used to ensure the requirements of the correct arc lengths are met. The algorithm is compared with its simplified version where equidistant spacing of the parametrization parameter is considered.

Keywords: Robotic manipulators, kinematics, singularities, trajectory planning, parametrization.

1. INTRODUCTION

In the present the Non-Destructive Testing technology is beginning to play an important role with regard to increasing the reliability of devices. This is especially true in the applications where defects in material from which the individual parts of technology are made can bring entire technology to the safety-critical situation. In manufacturing, welding process is commonly used for joining different parts of technology (armatures, fittings, pipes, pumps, heat exchanger, boilers, etc.). Therefore welds may encountered fatigue during their lifetime. This fatigues can be caused especially inappropriate conditions during welding process, e.g. base material must reach a certain temperature, must cool at the specific rate, must be welded witch adequate and compatible materials. In the opposite case the welding joint may not be strong enough to hold the parts together or some cracks may appear within the weld which may lead for example to break of components or to rupture of the pipes.

There are many technologies concerning NDT. They are based on the following principles: industrial radiography or industrial CT scanning using X-rays or gamma rays, ultrasonic testing, liquid penetrant testing, magnetic particle inspection or via eddy current. The ultrasonic testing is this one which will be used for proposed application. On the other hand, ultrasonic NDT technology is not the main focus of the paper. For more information about ultrasonic NDT, see Mix and Paul E. Mix (2005), Blitz and Simpson (1996).

There are two basic approaches for handling of NDT transducer. Firstly, NDT is performed manually. It means that the ultrasonic transducer is guided by the operator. Indeed, that is currently the most common method. Although, this method is very simple it suffers from some disadvantages, for example: it is difficult to ensure sufficient accuracy and repeatability, the scanning process can be very time consuming, therefore operator may be exposed to a prolonged adverse effects (high temperature, dusty environments, toxic and poisonous vapors, radioactive radiation, etc.). Secondly, NDT is performed using robotic manipulator which greatly improves the above mentioned drawbacks. Common industrial 6DoF manipulators are often used for applications where they test easily accessible welds, e.g. standard NDT cell NSpect 210, see Genesis Systems Group (2012), where universal 6DoF KUKA industrial robot of type KR60HA is used or NDT inspection system with KUKA KR5 Arc HW robot, see Mineo et al. (2012). On the other hand, there can be found some results considering complex hyper-redundant robots which use special overdetermined kinematic architecture to deal with the welds in the very confined spaces. An introduction and review of the hyper-redundant snake-like robot can be found in Hirose and Yamada (2009), Liljebäck et al. (2012). Some applications of OC Robotics company (snake-arm robot for confined space) related to aerospace and aircraft research are available on Anscombe et al. (2006), Buckingham and Graham (2003).

The aim of our research is ultrasonic NDT of commonly found pipe welds of nuclear power plant technology, es-

pecially four types of welds: circumferential weld, longitudinal weld, elbow weld and branch weld, see Fig. 1. The
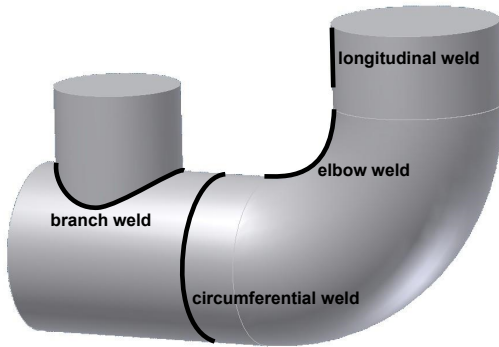

Fig. 1. Considered types of welds

above-mentioned common industrial robots can hardly be used because of free-space requirements for their installation which may be met in relation to nuclear power plant technology. On the other hand, hyper-redundant robots exhibit very complex kinematics, dynamics and control system algorithms. In addition, it is well known that the rigidity is one of the main drawbacks due to serial connections of many kinematic pairs. Therefore the snake-like robots are much more convenient for visual inspection purposes opposed to ultrasonic NDT where high accuracy of positioning of ultrasonic transducer is demanded. To overcome these inconveniences, there exists other type of robots of special kinematic architectures which are primary developed for ultrasonic NDT for pipe welds. These architectures are based on the simply, mostly 2DoF, manipulator which is attached to the pipe and performs circumferential motion around the pipe (1DoF) and usually 1DoF simple motion of ultrasonic transducer. But this type of manipulator suffers for its poor versatility because, in many cases, it is possible to use it only for very restricted set of welds and pipe diameters (usually only for one type of weld). In addition, many manipulators have to be accompanied by additional mechanical construction for circumferential motion associated with the specific type of weld , e.g. supporting chains, rails, etc. Fore some examples, see products of Force Technology (system *APS, ATS, AGS*), Force Technology (2013) and Olympus (system *WeldROVER*), Olympus, Inspection & Measurement Systems (2013).

The new kinematic architecture of universal 4DoF manipulator for ultrasonic NDT of pipe welds is introduced. The manipulator overcomes the drawbacks of above-mentioned single purposes NDT manipulators due to its versatility (4DoF, small space requirements) and makes possible to perform NDT for all type of pipe welds under consideration. The newly presented algorithm fo trajectory planning ensures required dimensions accuracy in the case of the branch weld which is known for its unnatural parametrization.

2. DESCRIPTION OF NEW MANIPULATOR

Special kinematic architecture of proposed manipulator is used in order to improve the universality and for possibility to use this manipulator for NDT applications regarding

wide range of welds. In addition, minimum possible size of the manipulator is required. For this purpose, the 4DoF manipulator of type **RRPR** was chosen, see Fig. 2. The proposed manipulator kinematic architecture was chosen as the best candidate from experiments regarding pipe welds inspection. In order to mount the ultrasonic transducer on the end-effector the position compensation is taken into account, see Fig. 3, where x_k, y_k, z_k is translation of the transducer coordinate system (CS) F_e with respect to end-effector CS F_4 and ϕ_k is its rotation about z_4 axis.
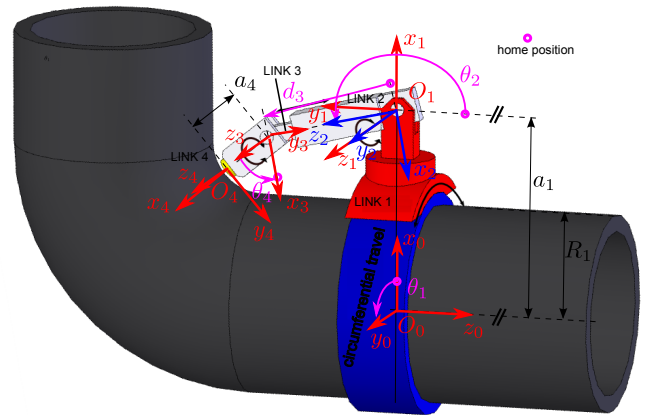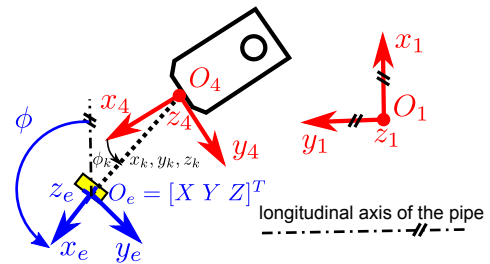

Fig. 2. Proposed 4DoF manipulator

Fig. 3. End-effector position compensation

2.1 Kinematics

The position of joint actuators are given as joint coordinates $\boldsymbol{Q} = [\theta_1, \theta_2, d_3, \theta_4]^T$, the position of the transducer X, Y, Z and its orientation ϕ represent general (task) coordinates $\boldsymbol{X} = [X, Y, Z, \phi]^T$. The design parameters of the manipulator are considered as the lengths of the links a_1 a_4 and transducer compensations x_k, y_k, z_k, ϕ_k outlining design parameters vector $\boldsymbol{\xi} = [a_1, a_2, x_k, y_k, z_k, \phi_k]^T$. Since the serial kinematic chain is considered the direct geometric model can be solved in the closed form with using well-known Denavit-Hartenberg notation, see Sciavicco and Siciliano (2000), Spong et al. (2005). The end-effector position is given as follows:

$$X = ((-y_k c_{\theta_4} + (-x_k - a_4)s_{\theta_4}) + d_3)s_{\theta_2} + \\ + ((x_k + a_4)c_{\theta_4} - s_{\theta_4}y_k)c_{\theta_2} + a_1)c_{\theta_1} - s_{\theta_1})z_k \quad (1)$$

$$Y = ((-y_k c_{\theta_4} + (-x_k - a_4)s_{\theta_4}) + d_3)s_{\theta_2} + \\ + ((x_k + a_4)c_{\theta_4} - s_{\theta_4}y_k)c_{\theta_2} + a_1)s_{\theta_1} + c_{\theta_1})z_k \quad (2)$$

$$Z = (-y_k c_{\theta_4} + (-x_k - a_4) s_{\theta_4}) + d_3) s_{\theta_2} -$$
$$- ((x_k + a_4) c_{\theta_4} - s_{\theta_4} y_k) s_{\theta_2} \quad (3)$$
$$\phi = \theta_2 + \theta_4 + \phi_k \quad (4)$$

where $s_\star = \sin(\star)$, $c_\star = \cos(\star)$.

The kinematic architecture of proposed manipulator even makes possible to solve inverse geometric model in the closed form. The position of joint coordinates depending on required transducer position are given:

$$\theta_1 = \text{atan2}\,(YV - Xz_k, XV + Yz_k) \quad (5)$$

where

$$V = \pm\sqrt{X^2 + Y^2 - z_k^2}$$

$$d_3 = \pm\sqrt{w_x^2 + w_y^2} \quad (6)$$

where

$$w_x = ((-x_k - a_4)c_\phi + s_\phi y_k)c_{\phi_k} +$$
$$+ (-c_\phi y_k - s_\phi(x_k + a_4))s_{\phi_k} + s_{\theta_1})Y - a_1 + Xc_{\theta_1}$$

$$w_y = (-c_\phi y_k - s_\phi(x_k + a_4))c_{\phi_k} +$$
$$+ ((x_k + a_4)c_\phi - s_\phi y_k)s_{\phi_k}) - Z$$

$$\theta_2 = \text{atan2}(\frac{w_x}{d_3}, \frac{-w_y}{d_3}) \quad (7)$$

$$\theta_4 = \phi - \theta_2 - \phi_k \quad (8)$$

It is clear that there exist four different solution of inverse geometric model, see equations (5), (6) but only positive solutions have to be taken into account for real manipulator. It can be shown, see 2.2, that for specific position of d_3 the manipulator is in singular configuration and solution of inverse geometric model degenerates - division by zero in (7) or the square root of a negative number in (5).

The forward (9) and inverse (10) instantaneous kinematic model can be derived as:

$$\dot{X} = J(Q)\dot{Q}, \quad \ddot{X} = \dot{J}(Q)\dot{Q} + J(Q)\ddot{Q} \quad (9)$$

$$\dot{Q} = J^{-1}(Q)\dot{X}, \quad \ddot{Q} = J^{-1}(Q)\left(\ddot{X} - \dot{J}(Q)\dot{Q}\right) \quad (10)$$

where kinematic jacobian $J = [j_{ij}]$, $i, j = 1 \ldots 4$ depending on joint coordinates Q is given as:(time derivative of $J(Q)$ is not introduced because of large number of terms):

$$j_{11} = 0.5(-d_3 c_{\bar{\theta}_{12}} + d_3 c_{\theta_{12}} - a_4 s_{\theta_{124}} - a_4 s_{\bar{\theta}_{124}}$$
$$- x_k s_{\theta_{124}} - x_k s_{\bar{\theta}_{124}} + y_k c_{\bar{\theta}_{124}} - y_k c_{\theta_{124}}) - c_{\theta_1} z_k - s_{\theta_1} a_1$$

$$j_{12} = 0.5(-a_4 s_{\theta_{124}} + a_4 s_{\bar{\theta}_{124}} + d_3 c_{\bar{\theta}_{12}} + d_3 c_{\theta_{12}}$$
$$- y_k c_{\bar{\theta}_{124}} - y_k c_{\theta_{124}} - x_k s_{\theta_{124}} + x_k s_{\bar{\theta}_{124}})$$

$$j_{13} = 0.5(s_{\theta_{12}} - s_{\bar{\theta}_{12}})$$

$$j_{14} = 0.5(-a_4 s_{\theta_{124}} + a_4 s_{\bar{\theta}_{124}} - y_k c_{\bar{\theta}_{124}} - y_k c_{\theta_{124}}$$
$$- x_k s_{\theta_{124}} + x_k s_{\bar{\theta}_{124}})$$

$$j_{21} = 0.5(d_3 s_{\theta_{12}} - d_3 s_{\bar{\theta}_{12}} + a_4 c_{\bar{\theta}_{124}} + a_4 c_{\theta_{124}}$$
$$- y_k s_{\theta_{124}} + y_k s_{\bar{\theta}_{124}} + x_k c_{\bar{\theta}_{124}} + x_k c_{\theta_{124}}) + c_{\theta_1} a_1 - s_{\theta_1} z_k$$

$$j_{22} = 0.5(-a_4 c_{\bar{\theta}_{124}} + a_4 c_{\theta_{124}} + d_3 s_{\theta_{12}} + d_3 s_{\bar{\theta}_{12}}$$
$$- y_k s_{\theta_{124}} - y_k s_{\bar{\theta}_{124}} - x_k c_{\bar{\theta}_{124}} + x_k c_{\theta_{124}})$$

$$j_{23} = 0.5(c_{\bar{\theta}_{12}} - c_{\theta_{12}})$$

$$j_{24} = 0.5(-a_4 c_{\bar{\theta}_{124}} + a_4 c_{\theta_{124}} - y_k s_{\theta_{124}} - y_k s_{\bar{\theta}_{124}}$$
$$- x_k c_{\bar{\theta}_{124}} + x_k c_{\theta_{124}})$$

$$j_{31} = 0, \ j_{32} = y_k s_{\theta_{24}} - x_k c_{\theta_{24}} - a_4 c_{\theta_{24}} - s_{\theta_2} d_3, \ j_{33} = c_{\theta_2},$$
$$j_{34} = -a_4 c_{\theta_{24}} - x_k c_{\theta_{24}} + y_k s_{\theta_{24}}$$

$$j_{41} = 0, \quad j_{42} = 1, \quad j_{43} = 0, \quad j_{44} = 1 \quad (11)$$

where $\theta_{124} = \theta_1 + \theta_2 + \theta_4$, $\bar{\theta}_{124} = \theta_1 - \theta_2 - \theta_4$, $\theta_{12} = \theta_1 + \theta_2$, $\bar{\theta}_{12} = \theta_1 - \theta_2$, $\theta_{24} = \theta_2 + \theta_4$.

2.2 Singularity analysis

The analysis of singular configurations plays important role in the design of manipulator. It is necessary to solve singular configurations of the manipulator before its real mechanical construction and trajectory planing to avoid excessively large joint velocities for manipulator moving near this unwanted positions. The singular configurations of the serial manipulator in joint space can be found through kinematic jacobian $J(Q)$. The following holds for manipulator being in the singular configuration:

$$\det(J(Q)) = 0 \quad (12)$$

Substituting (11) to (12) and using the half-tangent substitution

$$x_i = \tan\left(\frac{\theta_i}{2}\right) \Rightarrow s_{\theta_i} = \frac{2x_i}{1 + x_i^2}, \ c_{\theta_i} = \frac{1 - x_i^2}{1 + x_i^2} \quad (13)$$

we get the polynomial equation of type:

$$P(x_2, d_3, x_4)d_3 = 0 \quad (14)$$

Note that singular configuration is independent of joint coordinate θ_1. Solving (14) and back substituting (13) two conditions in joint space for robot to be in the singular configuration are derived:

$$d_3 = \frac{1}{s_{\theta_2}}(-x_k c_{\theta_2} c_{\theta_4} - c_{\theta_2} c_{\theta_4} a_4 + y_k s_{\theta_2} c_{\theta_4} + y_k c_{\theta_2} s_{\theta_4} - a_1$$
$$+ x_k s_{\theta_2} s_{\theta_4} + s_{\theta_2} s_{\theta_4} a_4) \quad (15)$$
$$d_3 = 0 \quad (16)$$

But for trajectory planing purposes it is much more efficient to show the singular positions of manipulator not only in joint space but also in general space (end-effector task space). For singularity of type 1, substituting the condition (15) to translation part of direct geometric model (1-3) and using (4) the following coordinates of the end-effector point are derived:

$$X = -s_{\theta_1} z_k, \quad Y = c_{\theta_1} z_k$$
$$Z = \frac{-(x_k c_{\theta_4} + c_{\theta_4} a_4 - s_{\theta_4} y_k + a_1 c_{\theta_2})}{s_{\theta_2}}$$

It can be shown by eliminating θ_1 that first two terms are fulfilled for end-effector point laying on the circle in XY plane of radius z_k. Z coordinate can be chosen arbitrary due to its dependency on θ_2, θ_4. So, the implicit form of the variety in task space is given in (17). It is dependent on design parameters z_k and forming the cylinder with longitudinal axis in z direction and radius z_k.

$$X^2 + Y^2 = z_k^2, \quad Z \in \mathbb{R} \text{ (arbitrary)} \quad (17)$$

For the singularity of type 2, similar substitution can be performed for the condition (16) and the following coordinates of the end-effector point are obtained:

$$X = c_{\theta_1}(a_4 c_{\phi-\phi_k} - y_k s_{\phi-\phi_k} + x_k c_{\phi-\phi_k}) - s_{\theta_1} z_k + c_{\theta_1} a_1$$
$$Y = s_{\theta_1}(a_4 c_{\phi-\phi_k} - y_k s_{\phi-\phi_k} + x_k c_{\phi-\phi_k}) + c_{\theta_1} z_k + s_{\theta_1} a_1$$
$$Z = -a_4 s_{\phi-\phi_k} - y_k c_{\phi-\phi_k} - x_k s_{\phi-\phi_k}$$

The joint coordinate θ_1 can be eliminated squaring and summing the first two terms. Therefore, for singularity of type 2, the implicit form of the variety in task space is given in (18). It can be easily seen that the variety is circle in XY plane with radius r and z-direction length Z. The radius and length is parametrized by required orientation of the end-effector ϕ and dependent on constant design parameters ξ.

$$X^2 + Y^2 = r$$
$$Z = -a_4 s_{\phi-\phi_k} - y_k c_{\phi-\phi_k} - x_k s_{\phi-\phi_k} \qquad (18)$$

where $r = (x_k + a_4 + y_k)(x_k + a_4 - y_k)c_{\phi-\phi_k}^2 + 2(x_k + a_4)(-y_k s_{\phi-\phi_k} + a_1)c_{\phi-\phi_k} + z_k^2 - 2y_k s_{\phi-\phi_k} a_1 + y_k^2 + a_1^2$.

Both singularities are depicted in Figs. 4, 5. For singularity of type 1 the motion of manipulator is blocked for the end-effector direction perpendicular to $x_1 y_1$ plane. For singularity of type 2 (actuator d_3 is fully retracted) the motion of manipulator is generally blocked for the end-effector direction laying in $x_1 y_1$ plane. These singular configurations should be rigorously considered when implementing trajectory generators.
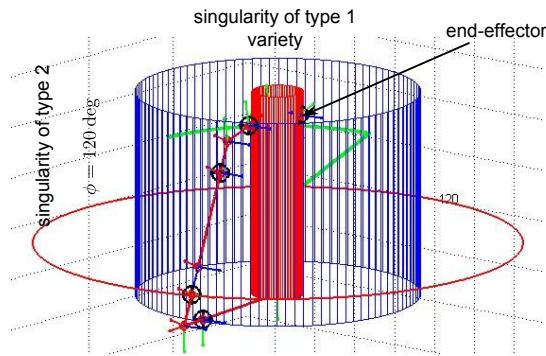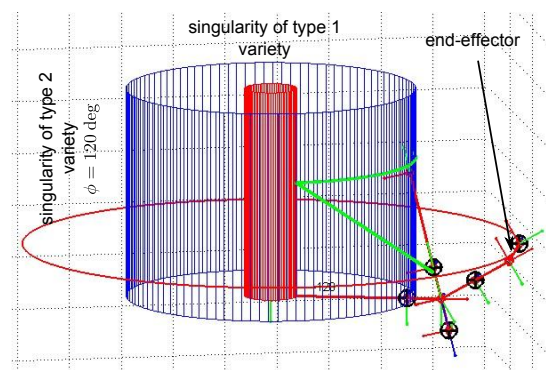

Fig. 4. Singularity of type 1 in SimMechanics

Fig. 5. Singularity of type 2 (parametrized by ϕ) in SimMechanics

3. TRAJECTORY GENERATORS

The trajectory generators are supposed to give position, velocity and acceleration of the end-effector motion for four considered welds. There are two approaches to perform ultrasonic NDT. The first one is to use standard (one or several beams) ultrasonic transducer and so the meandering motion along the scanning weld have to be used (measuring motion is perpendicular to the weld). The other one uses advanced phased array ultrasonic transducer where the meandering motion can be replaced by simple motion along the weld, see Fig. 6. It is achieved through using multiple ultrasonic elements and electronic time delays to create beams that can be steered, scanned, swept, and focused electronically.
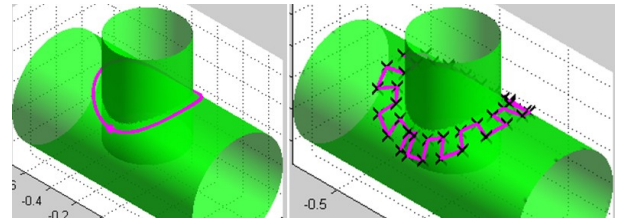

Fig. 6. An example of simple and meandering motion of branch weld

It can be shown that the circumferential, longitudinal and elbow welds consist of primitive geometric entities such as line and circle. It is generally known that arc length of these primitives can be computed analytically. In addition, for known parametrization of the lines and arcs, it is possible to compute relation between arc length and parameters of these entities analytically. It makes possible to compute correct position, velocity and acceleration of the end-effector of manipulator as soon as the length $s(t)$, velocity $v(t)$ an acceleration $a(t)$ profile for point moving along parametrized trajectory is known. For more information about algorithms for trajectory generators of welds mentioned above, see Švejda (2013).

However, it is getting to be more difficult if we consider the branch weld. This type of trajectory is given by an intersection of two perpendicular cylinders (known as Steinmetz solid). We suppose continuous pipe V_2 of radius R_2 and adjoining pipe V_1 of radius R_1 for $R_1 \leq R_2$. The manipulator is placed around the pipe V_1 and the home position of moving base ($\theta_1 = 0$) coincides with direction of x_0-axis. The translation and orientation of longitudinal pipe V_2 is defined via distance z_{0k} and angle γ, see Fig. 7. The next parameters defining the branch weld trajectory are supposed as: d distance between sweep segments along the intersection of pipes, L length of sweep segments, c distance of sweep segments from intersection of pipes, N distance between generated points of trajectory (resolution of the algorithm) and ϕ_{start} starting angle for trajectory generation (with respect to base frame). For the beginning, we assume $c = 0$, so the required simple trajectory (without sweeping) is given by the parametrization of Steinmetz solid:

$$\begin{bmatrix} X \\ Y \\ Z \end{bmatrix} = \mathbf{\Phi}(\phi) = \begin{bmatrix} \cos(\gamma) R_1 \cos(\phi) - \sin(\gamma) R_1 \sin(\phi) \\ \sin(\gamma) R_1 \cos(\phi) + \cos(\gamma) R_1 \sin(\phi) \\ \sqrt{R_2^2 - R_1^2 + R_1^2 (\sin(\phi))^2} + z_{0k} \end{bmatrix}$$

$$(19)$$

where $\varphi \in \mathbb{R}$ is parameter.

Unfortunately, it can be shown that (19) is not a natural parametrization. Therefore the equidistant spacing of parameter ϕ do not generate equidistant spacing of arc
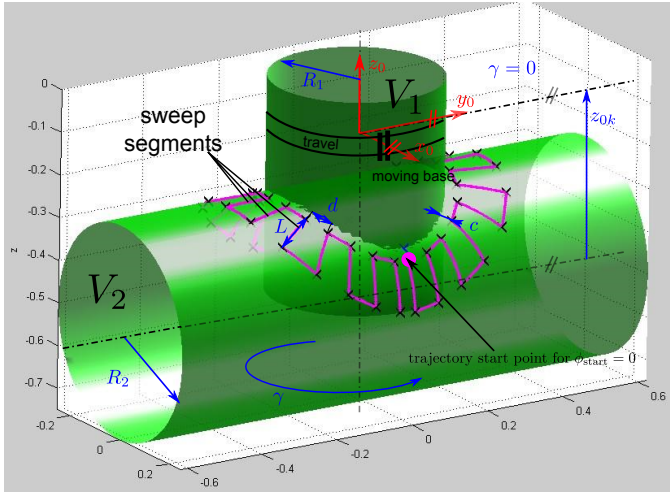
Fig. 7. Branch weld meandering motion

length $s(\phi)$. In addition, it is not possible to compute arc length $s(\phi)$ analytically because the solution of the integral function (20) does not exist in closed form.

$$s(\phi) = \int_0^\phi \sqrt{\left(\frac{\partial \mathbf{\Phi}}{\partial \phi}\right)^T \cdot \frac{\partial \mathbf{\Phi}}{\partial \phi}} \, d\phi = \int_0^\phi \left\| \frac{\partial \mathbf{\Phi}}{\partial \phi} \right\| d\phi \quad (20)$$

3.1 Equidistant spacing of sweep segments

In order to fulfill the requirements on equidistant spacing d of sweep segments the problem can be reformulated to finding a suitable sequence of discreet values of ϕ. One of the possible methods based on Taylor expansion of $\phi(t)$, see Constantinescu (1998), can be used in the following manner. The time dependency between velocity $\frac{ds(t)}{dt}$ along the trajectory and time derivative $\frac{d\phi(t)}{dt}$ of ϕ can be derived from (20):

$$\frac{ds}{dt} = \frac{ds}{d\phi} \cdot \frac{d\phi}{dt} \text{ and } \frac{ds}{d\phi} = \left\| \frac{\partial \mathbf{\Phi}}{\partial \phi} \right\| \Rightarrow \frac{d\phi}{dt} = \frac{1}{\left\| \frac{\partial \mathbf{\Phi}}{\partial \phi} \right\|} \cdot \frac{ds}{dt} \quad (21)$$

It holds for the second time derivatives:

$$\frac{d^2\phi}{dt^2} = \frac{1}{\left\| \frac{\partial \mathbf{\Phi}}{\partial \phi} \right\|} \cdot \left[\frac{d^2s}{dt^2} - \frac{\left(\frac{\partial \mathbf{\Phi}}{\partial \phi}\right)^T \cdot \frac{\partial^2 \mathbf{\Phi}}{\partial \phi^2} \cdot \left(\frac{ds}{dt}\right)^2}{\left\| \frac{\partial \mathbf{\Phi}}{\partial \phi} \right\|^3} \right] \quad (22)$$

The second order Taylor expansion of $\phi(t)$ can be expressed using (21, 22) for discreet time intervals $t_k = T_S \cdot k$, $k = 0, 1, \ldots$ and sample period T_S as:

$$\phi(t_{k+1}) = \phi(t_k) + \frac{d\phi}{dt}\big|_{t=t_k} \cdot T_S + \frac{1}{2}\frac{d^2\phi}{dt^2}\big|_{t=t_k} \cdot T_S^2 + O(T_S^3) \quad (23)$$

Now, we denote $\frac{ds}{dt} = V(t)$ a $\frac{d^2s}{dt^2} = A(t)$ as required velocity and acceleration of the arc length along the trajectory and assume constant velocity $V(t) = V = const. \Rightarrow A(t) = 0$. The equation (23) can be rewritten as:

$$\phi(t_{k+1}) \approx \phi(t_k) +$$
$$+ \frac{1}{\left\| \frac{\partial \mathbf{\Phi}}{\partial \phi} \right\|} \cdot \left[V \cdot T_S - \frac{\left(\frac{\partial \mathbf{\Phi}}{\partial \phi}\right)^T \cdot \frac{\partial^2 \mathbf{\Phi}}{\partial \phi^2}}{2\left\| \frac{\partial \mathbf{\Phi}}{\partial \phi} \right\|^3} \cdot V^2 \cdot T_S^2 \right] \quad (24)$$

And the term $V \cdot T_S$ expresses traveled distance along trajectory in time T_S for constant velocity V. Therefore, the following substitution can be performed $V \cdot T_S = N$, where N is differential traveled distance between two consecutive points on the trajectory or, in the other words, the resolution of trajectory generation mentioned above. From Taylor expansion it is clear that the accuracy of the approximation of the parameter ϕ is given by the Taylor's remainder $O(N^3)$ for each step k. This brings the main drawback of proposed algorithm due to summing approximation errors. But the error can be neglected for relatively small number of iteration steps. The inversion of (20) can be computed numerically from (24) as follows:

(1) Initialize: $\phi_0 = \phi_{start}$
(2) Iterate (25) through $k = 0 \ldots n$:

$$\phi_{k+1} = \phi_k + \frac{1}{\left\| \frac{\partial \mathbf{\Phi}}{\partial \phi} \right\|} \cdot \left[N - \frac{\left(\frac{\partial \mathbf{\Phi}}{\partial \phi}\right)^T \cdot \frac{\partial^2 \mathbf{\Phi}}{\partial \phi^2}}{2\left\| \frac{\partial \mathbf{\Phi}}{\partial \phi} \right\|^3} \cdot N^2 \right] \quad (25)$$

(3) $\phi = \phi_n$

where N is chosen resolution of the algorithm, ϕ_{start} is the starting point on the trajectory (19), $n = \left[\frac{S}{N}\right]$ where S is required arc length along the trajectory (e.g. $S = d$ to ensure equidistant spacing of sweep segments) and $[\star]$ denotes integer division operator. Computed value of ϕ corresponds to required arc length S which is traveled along trajectory (19) from starting parameter point ϕ_{start} to ϕ resulting to $\Delta\phi = \phi - \phi_{start}$ (generally non-equidistant increments of parameter of given trajectory parametrization).

The algorithm (25) is used for computing of the points where the sweeping is required along the branch weld trajectory. If one point of the sweeping is known, e.g. $\mathbf{A} = \mathbf{\Phi}(\phi_A)$, the following point, e.g. $\mathbf{B} = \mathbf{\Phi}(\phi_B)$ which is at a distance d along the trajectory, is given by (25) for $\phi_{start} = \phi_A$, $\phi_B = \phi$ and $S = d$. The accuracy of the proposed algorithm is compare with simplified algorithm. The simplified algorithm suppose that the branch weld is given only by the circle of radius R_1. Therefore the parameter ϕ is generated equidistantly with $\Delta\phi = \frac{d}{R_1}$. The increments $\Delta\phi_i$ for i-th sweep segment given by the algorithm (25) (non-equidistant) and simplified algorithm (equidistant) are used for the computing of the parameter ϕ from the trajectory parametrization (19) as:

$$\phi_i = \phi_{start} + \sum_{i=1,2,\ldots} \Delta\phi_i \quad (26)$$

The parameter ϕ_i can be recomputed back into arc length $d_i^\star = \int_{\phi_i}^{\phi_{i+1}} \sqrt{\left(\frac{\partial \mathbf{\Phi}}{\partial \phi}\right)^T \cdot \frac{\partial \mathbf{\Phi}}{\partial \phi}} \, d\phi$ of the trajectory (19) using adaptive Simpson quadrature, Gander and Gautschi (2000) (numerical calculation of the integral (20) with given relative accuracy, here 10^{-10} is used). The maximum absolute and relative error are given as $e_{abs}[m] = max_i \|d_i^\star - d\|$ and $e_{rel}[\%] = 100\frac{e_{abs}}{d}$. The branch weld parameters are supposed as $R_1 = 0.3m$, $R_2 = 0.35m$, $z_{0k} = -0.8m$, $\gamma = 0rad$, $d = 0.03m$, $N = 0.006m$. For simplified algorithm the errors are $e_{abs} = 4.6mm$, $e_{rel} = 15.3\%$ and the variance $Var(d_i^\star) = 4.45mm$ and

for proposed algorithm $e_{\text{abs}} = 0.005mm$, $e_{\text{rel}} = 0.02\%$ and $\text{Var}(d_i^\star) = 0.01mm$.

3.2 Equidistant length and distance of sweep segments

The similar problem arises when the equidistant length L of sweep segments and its distance c from cylinder intersection (19) have to be fulfilled. It can be shown that the trajectories of sweep segments consist of ellipses (the intersection of a cylinder and sweeping plane) with the following parametrization:

$$\begin{bmatrix} X \\ Y \\ Z \end{bmatrix} = \mathbf{\Phi}(\psi) = \begin{bmatrix} b\sin(\psi)(\cos(\gamma)\cos(\phi) - \sin(\gamma)\sin(\phi)) \\ b\sin(\psi)(\sin(\gamma)\cos(\phi) + \cos(\gamma)\sin(\phi)) \\ a\cos(\psi) + z_{0k} \end{bmatrix} \quad (27)$$

where ϕ defines the point of sweeping around the branch weld trajectory, ψ is a parameter and $a = R_2$, $b = \frac{R_2}{\|\cos(\phi)\|}$.

It is well known that there does not exist any natural parametrization of an ellipse. Therefore proposed algorithm mentioned above can be used for computing the values of the parameter ψ. Assume that the parameter ψ_{start} corresponding to the point laying on cylinder intersection for given ϕ (sweep segment) is known. Then the parameter ψ_c corresponding to the point on sweep segment at the distance c along ellipse trajectory is given analogously through algorithm (25) where ϕ is substituted by ψ, $\mathbf{\Phi}$ is the parametrization (27) and $S = c$. The parameter ϕ_{c+L} corresponding to the point on sweep segment at the distance $c+L$ along ellipse trajectory is given by the same algorithm for $\psi_{start} = \psi_c$ and $S = L$.

4. CONCLUSION

The new robotic architecture of NDT robot for pipe welds is presented. The proposed architecture is designed in order to reduce space requirements as well as makes possible to deal with more complex welds. The kinematic analysis is studied in section 2. There is shown that inverse geometric model can be solved in the closed form. The singularity analysis is based on the knowledge of jacobian matrix and two types of singularities exist. These singularities can be easily derived in joint space resulting in the specific positions of prismatic actuator. It is much more convenient to transform the singularities to general space (task space) which leads to the finding two varieties in the XYZ task space. Therefore the possibility that the manipulator approaches close to the singular configurations can be minimized during the trajectory planning algorithm.

The trajectory planning is presented in section 3. Four geometries of pipe welds are introduce. It can be shown that there is no problem with circumferential, elbow and longitudinal welds including simple and meandering motion because of possibility to parametrize these geometric primitives naturally. On the other hand the parametrization of branch weld leads to unnatural parametrization because of the presence of the primitives like ellipses and Steinmetz solid. Therefore the new numerical algorithm for computing the parametrization parameter is presented to ensure the required arc length of individual trajectory segments (spacing, distance and length of sweep segments). The proposed algorithm is computationally efficient and

the relative error of arc length gained through computed parameter is approximately 0.02% for expected branch weld size.

REFERENCES

Anscombe, R., Bryant, A and, B.R., Ferguson, G., and et al. (2006). Snake-arm robots: A new approach to aircraft assembly. *SAE Technical Paper 2006-01-3141*. doi:doi:10.4271/2006-01-3141.

Blitz, J. and Simpson, G. (1996). *Ultrasonic Methods of Non-destructive Testing*. Non-Destructive Evaluation Series. Springer. URL http://books.google.cz/books?id=d3WWect9zQEC.

Buckingham, R. and Graham, A. (2003). Snake-arm robots ? a new tool for the aerospace industry. *SAE Technical Paper 2003-01-2952*. doi:10.4271/2003-01-2952.

Constantinescu, D. (1998). *Smooth Time Optimal Trajectory Planning for Industrial Manipulators*. Ph.D. thesis, THE UNIVERSITY OF BRITISH COLUMBIA.

Force Technology (2013). *Force Technology - General application scanners*. http://www.forcetechnology.com/en/Menu/Products/P-scan/Scanners/General/.

Gander, W. and Gautschi, W. (2000). Adaptive quadrature revisited. *BIT Numerical Mathematics*, 40(1), 84–101. doi:10.1023/A:1022318402393. URL http://dx.doi.org/10.1023/A%3A1022318402393.

Genesis Systems Group, L. (2012). *Robotic Non-Destructive Inspection NSpect 210*. www.genesis-systems.com.

Hirose, S. and Yamada, H. (2009). Snake-like robots [tutorial]. *Robotics Automation Magazine, IEEE*, 16(1), 88–98. doi:10.1109/MRA.2009.932130.

Liljebäck, P., Pettersen, K., Stavdahl, O., and Gravdahl, J. (2012). A review on modelling, implementation, and control of snake robots. *Robotics and Autonomous Systems*, 60(1), 29 – 40. doi:http://dx.doi.org/10.1016/j.robot.2011.08.010.

Mineo, C., Herbert, D., Morozov, M., and Pierce, S.G. (2012). Robotic non-destructive inspection. In *51st Annual Conference of the British Institute of Non-Destructive Testing 2012*, 345–352.

Mix, P. and Paul E. Mix, P.E., E. (2005). *Introduction to Nondestructive Testing: A Training Guide*. Wiley. URL http://books.google.cz/books?id=cXWU-jsgS54C.

Olympus, Inspection & Measurement Systems (2013). *WeldROVER Scanner*. http://www.olympus-ims.com/en/scanners/weldrover/.

Sciavicco, L. and Siciliano, B. (2000). *Modelling and Control of Robot Manipulators*. Springer, 2 edition.

Spong, M.W., Hutchinson, S., and Vidyasagar, M. (2005). *Robot Modeling and Control*. Wiley, 1 edition.

Švejda, M. (2013). Manipulator pro NDT (varianta 2: RRPR manipulator). URL http://home.zcu.cz/~msvejda/_publications/2013/7_UJV_genTraj.pdf.